BNL-105678-2014-TECH

BNL/SNS Technical Note No. 110;BNL-105678-2014-IR

A Large-Aperture Narrow Quadrupole for the SNS Accumulator Ring

N. Tsoupas

March 2002

Collider Accelerator Department

Brookhaven National Laboratory

U.S. Department of Energy

USDOE Office of Science (SC)

DISCLAIMER

A Large-Aperture Narrow Quadrupole for the SNS Accumulator Ring

BNL/SNS TECHNICAL NOTE

NO. 110

N. Tsoupas, J. Brodowski, W. Meng, J. Wei and Y.Y. Lee

March 21, 2002

COLLIDER-ACCELERATOR DEPARTMENT
BROOKHAVEN NATIONAL LABORATORY
UPTON, NEW YORK 11973

Accelerator Division
Collider Accelerator Department
Brookhaven National Laboratory
Upton, NY 11973

A Large-Aperture Narrow Quadrupole for the SNS Accumulator Ring

N Tsoupas, J. Brodowski, W. Meng, J. Wei, and Y.Y. Lee

March 21 2002

Abstract

The accumulator ring of the Spallation Neutron Source (SNS) [1] is designed to accept high-intensity H^- beam of 1 GeV kinetic energy from the injecting LINAC, and to accumulate, in a time interval of 1 msec, $2x10^{14}$ protons in a single bunch of 700 nsec,. In order to optimize the effective straight-sections spaces for beam-injection [2], extraction [3] and collimation[4], we have minimized the width of the large aperture (Radius=15 cm) quadrupoles which are located in the same straight sections of the accumulator ring where the injection and extraction systems are located. The minimization of the quadrupole's width to ±40.4 cm allows for low values for beam-injection and beam-extraction angles. For this particular design of the narrow quadrupole, (also known as "figure-of-8" quadrupole), the beam-injection and beam-extraction angles are lowered to 8.75^o and 16.8^o respectively. Further optimization of the narrow quadrupole, minimizes the strength of the dodecapole multipole component of the quadrupole, thus decreasing the width of the 12pole structured resonance and allowing a larger tune space for beam stability[5].
In this paper we present results derived from magnetic field calculations of 2D and 3D modeling and discuss the method of optimizing the size of the quadrupole and minimizing its dodecapole multipole component.

Why Use Narrow Quadrupole?

The SNS accumulator ring[1], shown schematically in Fig. 1, is 248 m in length and consists of four identical arcs of 90^o each. The arcs are connected by four straight sections, each 31.5m in length. As part of the ring's beam optics a set of two quadrupole-doublets are located along each of the straight sections (see Fig. 1), and placed symmetrically with respect to the center of each straight section.
The presence of the quadrupole doublets in the straight sections of the ring where the beam-injection and beam-extraction systems are located (see Fig. 1), suggests that the dimensions of the quadrupoles determine the various parameters of the magnets in the beam-injection and extraction systems.
A more detail view of the injection region is shown in Fig. 2 which shows the quadrupole doublets, the injection septum, and the four chicane dipole magnets which generate the local orbit bump[2] necessary to displace the closed orbit at the location of the striping foil. In order to minimize the magnetic-field-stripping of the H^- beam or the H^0

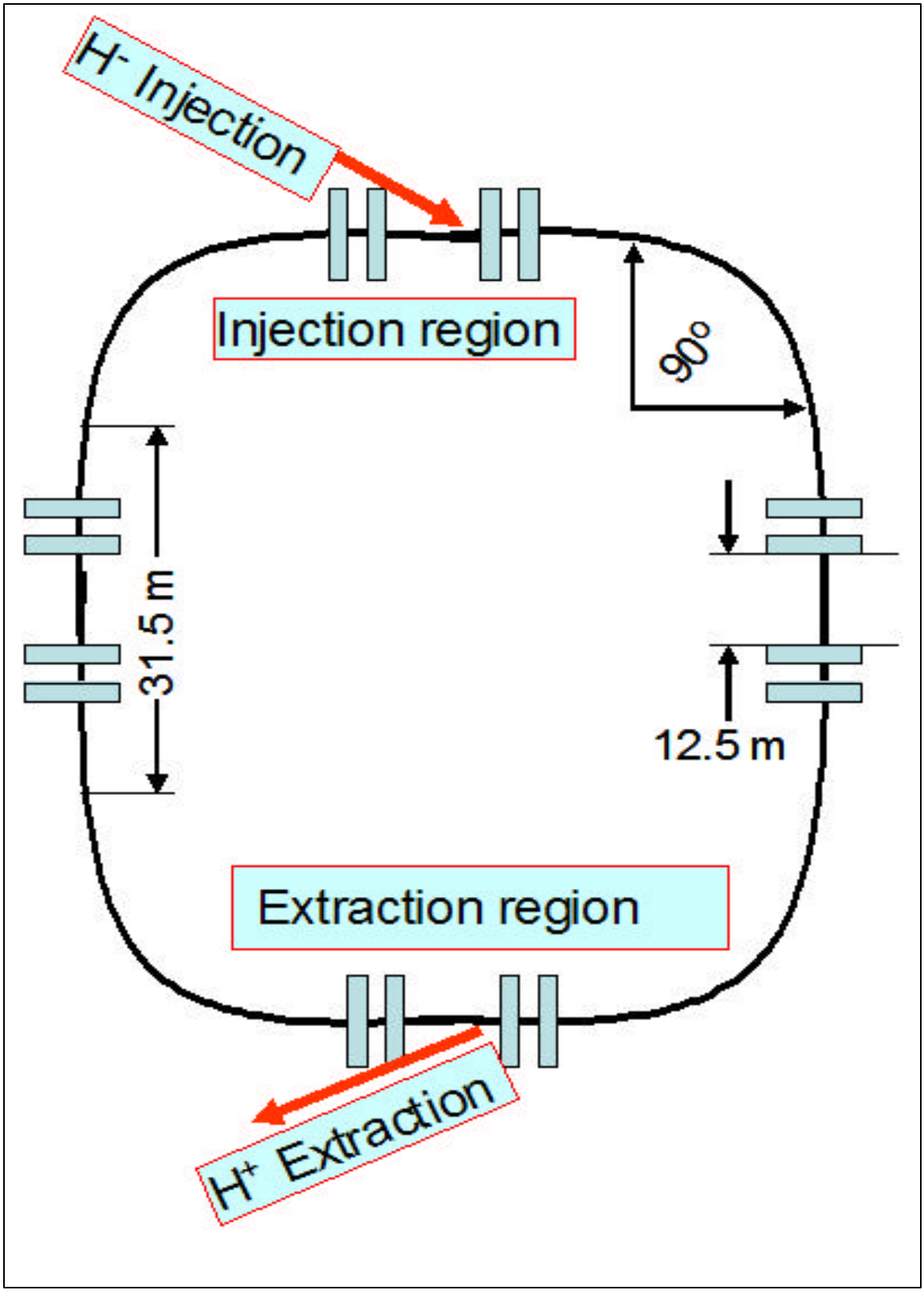

Figure 1 Schematic diagram of the SNS accumulator ring showing the four 90^{o} arcs, the the four straight sections of the ring the injection and extraction regions and the location of the narrow quadrupole doublets.

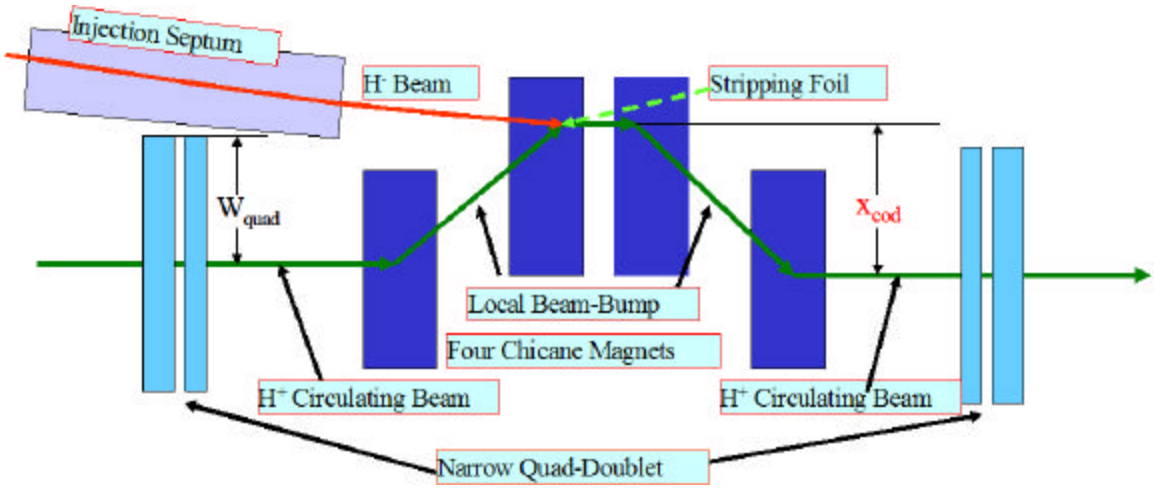

Figure 2 Schematic diagram of the injection region showing the four chicane magnets which generate the local injection orbit bump, the narrow quadrupoles and the injection septum magnet. The angle of beam injection is 8.75°.

beam [7] which is produced by the incomplete stripping of the H^- beam by the stripping foil, the chicane magnets should be excited at the lowest possible magnetic fields. Low excitation fields of the chicane magnets requires smaller size (x_{cod}) of the local orbit bump shown in Fig. 1. The size of (x_{cod}) can be reduced by moving the injection septum magnet closer to the ring and reducing also the transverse dimension W_{quad} of the quadrupoles which otherwise would interfere. Thus the narrow quadrupoles can accommodate a reduced size of the local bump (x_{cod}) which can be produced by lower field strength of the chicane magnets.
Similarly the quadrupole doublets which are located at the straight section where the beam-extraction system is located (see Fig. 3), interfere laterally with the extracted beam.

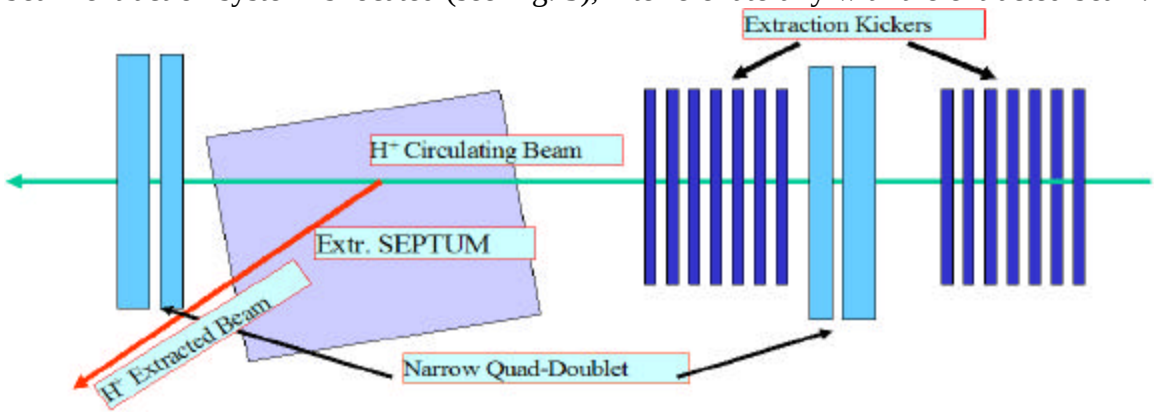

Figure 3. Schematic diagram of the extraction region showing the vertically-extraction kickers the horizontally-extraction septum abd the direction of the extracted beam passing by the narrow quadrupoles. The extraction angle is 16.8°.

Reduction of the quadrupole width reduces the beam extraction angle to 16.8° and allows lower excitation value of the B-field of the septum magnet thus reducing the effect of the fringing fields of the septum magnet on the circulating beam.

GEOMETRICAL AND MAGNETIC FIELD REQUIREMENTS OF THE NARROW QUADRUPOLE

The cross-section of the narrow quadrupole is shown in Fig. 4. The dark blue color designates the iron of the magnet and the red-colored regions designate the coils of the magnet.

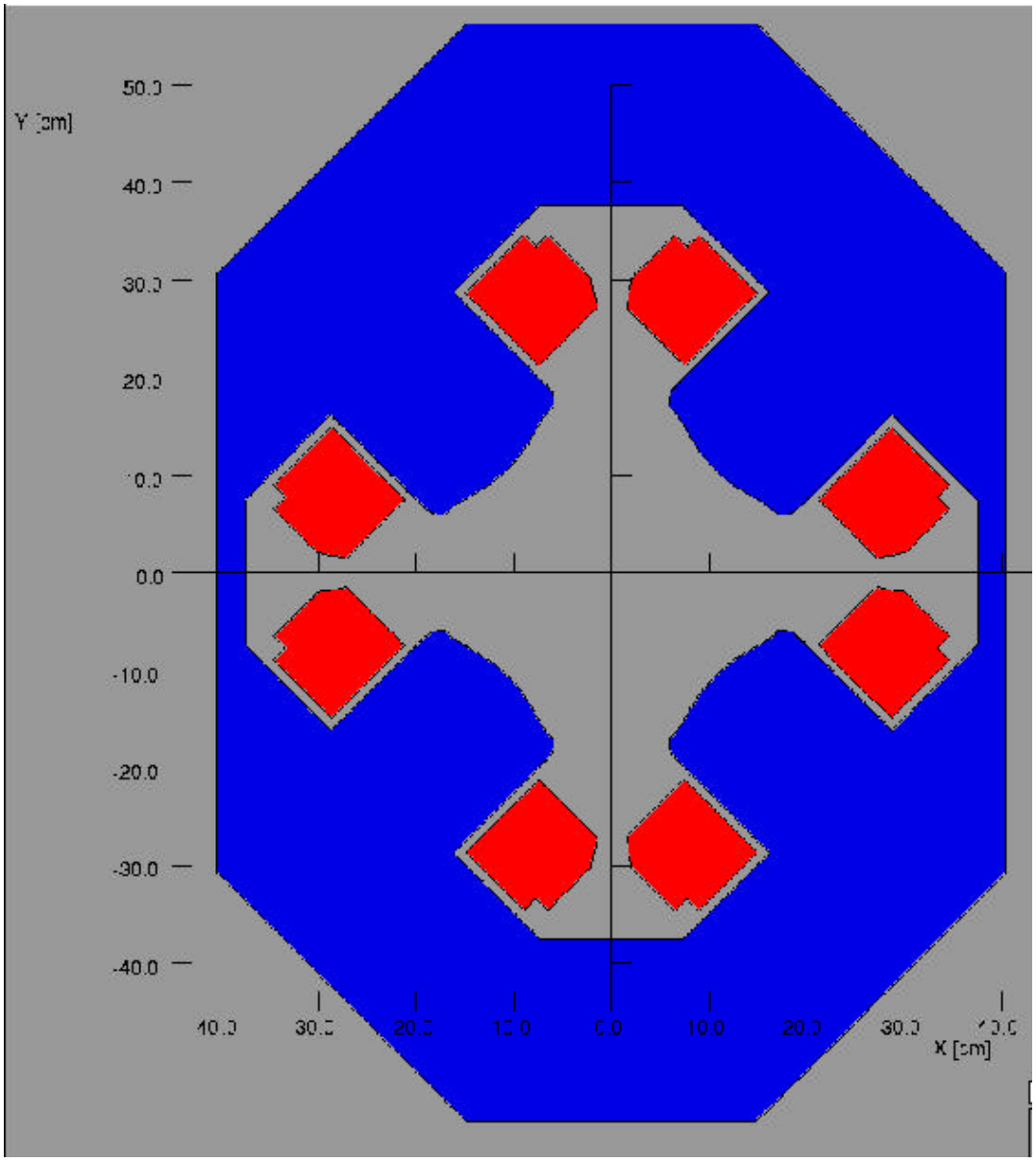

Figure 4. Cross section of the narrow quadrupole. The contour of the pole faces has been designed to minimize the strength of the 12-pole multipole. The strength of the fringe field generated by the quadrupole at distances x<-42 cm and x>42 cm is shown in figure 5, is small enough not to affect the 1.0 GeV extracted beam.

The dimensions of the narrow quadrupole magnets, which appear in Table 1, were determined from a) the size of the beam at the location of the quadrupoles, b) the allowed uncontrolled beam-losses along the ring[4] and c) the magnetic-field requirements of the quadrupoles. The length, the width, and pole-width of the quadrupole (columns 3,4,5 of Table 1) have been chosen to minimize the effects of magnetic field saturation on the magnet, and thus maintain the same field quality for 1.0 and 1.3 GeV operations. The transverse width of ±40.4 cm (column 4) of the quadrupoles allows for 8.75^{o} and 16.8^{o} beam-injection and beam-extraction angles.
The required B-field gradients for the 1.0 and 1.3 GeV operations appears in column 6, and the allowed magnetic field non-uniformity expressed as the ratio of the dodecapole field to the quadrupole field at a radius of 10 cm should be B_{dod}/B_{quad} 2×10^{-4}. This upper limit of the dodecapole multipole keeps the width of the resonance[5] away from the tune spread of the beam thus allowing for beam stability of the circulating beam.

Table 1: Dimensions and field requirements of the narrow quadrupoles of each doublet.

Name	R [cm]	L [cm]	W [cm]	PW [cm]	G[T/m]	B_{dod}/B_{quad}
30Q44	15	44	80.8	17.8	4.2 , 5.1	2×10^{-4}
30Q58	15	58	80.8	17.8	4.2 , 5.1	2×10^{-4}

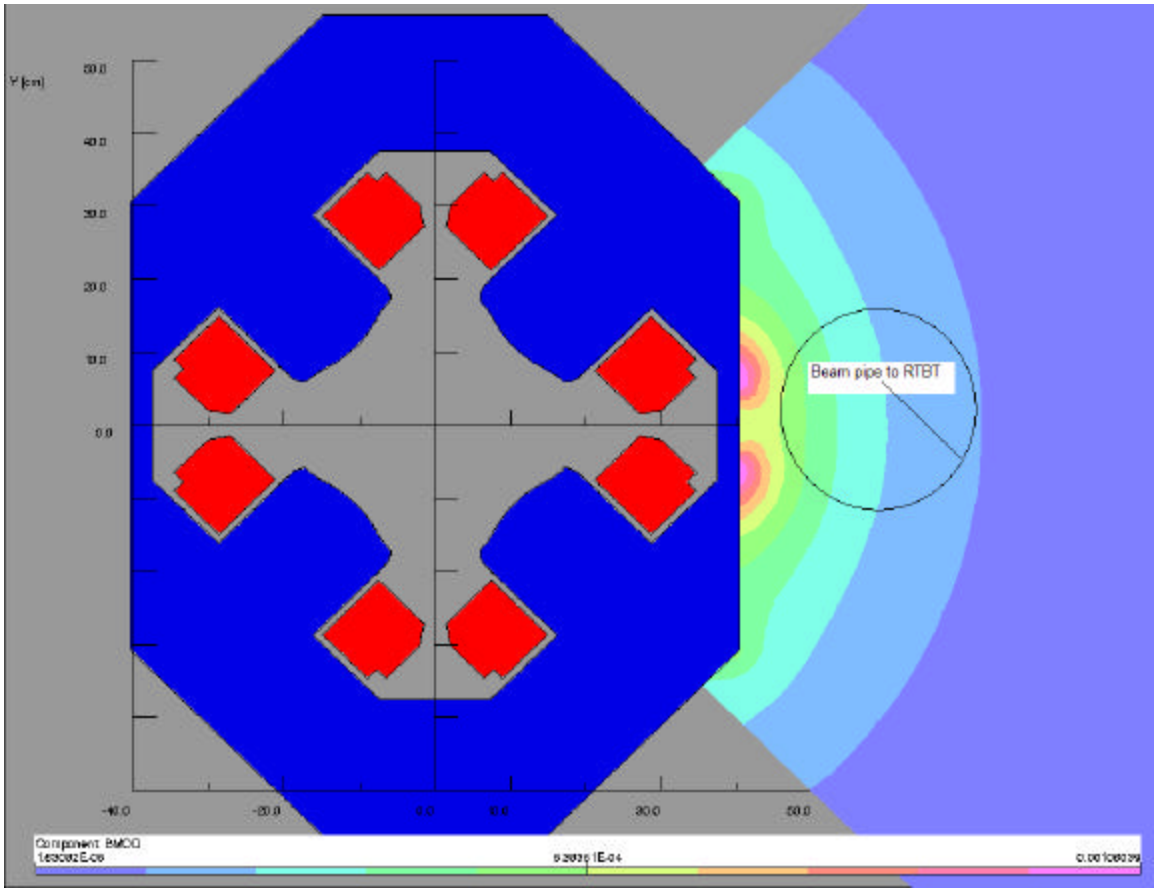

Figure 5 Contour plot of the value of the field Bmod at distances x>40.4 cm inside the RTBT vacuum pipe. The value of the field inside the pipe is ~5Gauss.

The fringe field of the quadrupole at distances x>40.4 cm is shown in figure 5. The strength of the field at distances ~10 cm from the iron, where the RTBT vacuum pipe passes, is small enough (see figure 5) not to affect the injected and extracted beams.

Magnetic Modeling of the Narrow-Quadrupole

The magnetic modeling of the narrow quadrupole was performed to determine a) the contour of the pole face, and b) the minimum dimensions of the width and pole-width of the magnet, that satisfy the field requirements of the magnet. The commercially available computer code "opera" of Vector-Fields Inc. [6] was used for the modeling of the magnet and was done in two steps; first 2D-modeling and second 3D modeling.

2D modeling

The 2D modeling establishes the contour of the pole-face that minimizes the dodecapole multipole[1]. The contour of the pole face that generates the multipoles shown in Table 2 is very simple and is described in Fig. 6 which contains the required coordinates of the points and the radii of curvatures to reproduce the contour.

Table 2: The strength of the allowed multipoles[2] b_n have been calculated within a radius of 15 cm for two excitations of the magnet at 1 GeV and 1.3 GeV.

T [GeV]	$b_{1\ quad}$ [$T*m^{-1}$]	$b_{3\ oct}$ [$T*m^{-3}$]	$b_{5\ duod}$ [$T*m^{-5}$]	$b_{7\ 16pole}$ [$T*m^{-7}$]	$b_{9\ 20pole}$ [$T*m^{-9}$]
1.0	4.236	$-1.1x10^{-4}$	2.20	-0.30	$-2.6\ x10^{5}$
1.3	5.081	$-2.2x10^{-4}$	-0.22	-0.67	$-3.1x10^{5}$

The 2D modeling establishes also the minimum width of the iron-pole (in this case 17.8 cm) that prevents strong magnetic field saturation effects in the iron. Indeed Table 2 shows that, the multipoles do not vary linearly with the quadrupole strength. However the strength of the multipoles (higher than the quadrupole) shown in Table 2, for the excitation energies of 1.0 and 1.3 GeV operations is too small to affect the field quality of the magnet.

The ratio B_{dod}/B_{quad} at r=10 can be calculated from the data in Table 2 and is $2x10^{-4}$ as required. The absolute value of the magnetic field B_{mod} in the iron is shown in Fig.7 and its maximum value is below the saturation level ~17kG.

The width of the magnet is 80.8 cm and allows for enough space to accommodate the conductors of the quadrupole, and power them with reasonable current density for the 1.3 GeV operation.

The 2D modeling is a quick method to optimize the magnets's transvers dimensions and to define the contour of the pole faces of the magnet which should satisfy the field requirements only well inside the magnet where the longitudinal field component B_z is negligible.

---

[1] The symmetry of this "narrow-quad" is not four-fold symmetric therefore the duodecapole multipole is not the first allowed multipole (Table 2). However the strength of the allowed multipoles introduced due to the break of the four fold symmetry of the quad are negligible as shown in Table 2.

[2] The strength b_n of a multipole is defined from the expansion of the radial field B_r as:
$B_r = \Sigma b_n r^n \cos[(n+1)\theta]$ {n=0 for dipole-field, n=1 for Quad…..}

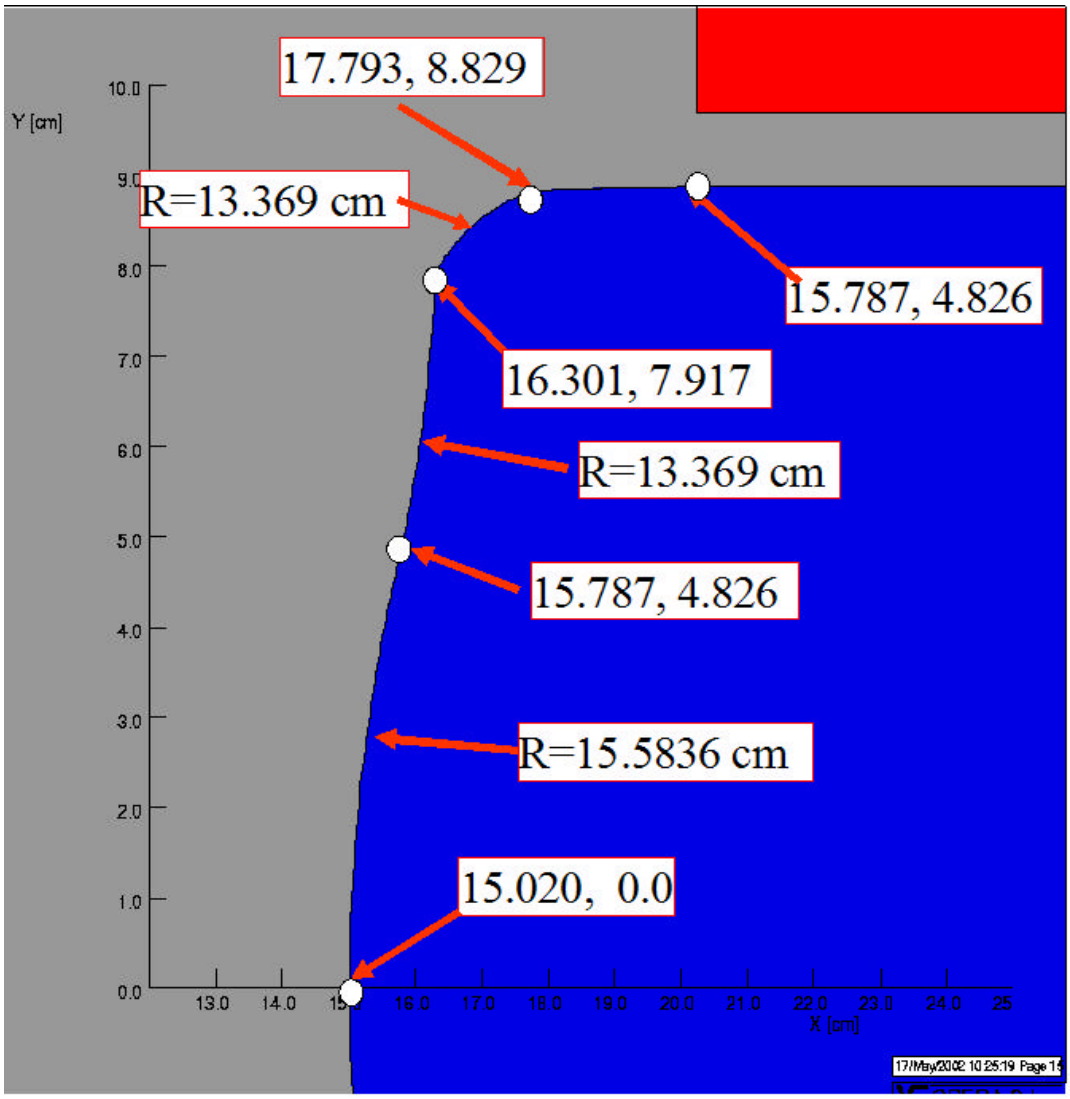

Figure 6 The coordinates in [cm] and the radii of curvature required to generate the contour of the pole face of the quad that generates the multipoles shown in Table 2.

3D modeling

The 3D modeling provides complete information about the magnetic field of the magnet in 3D space and helps further in the optimization of the shape of the magnet which should satisfy all the magnetic field requirements. The 3D model of a 44 cm long quadrupole was generated by using the same cross section as the cross section of an optimized quadrupole from 2D calculations describe earlier, and the 3D magnetic field calculations have been performed using the TOSCA module of the opera computer code[6].
The aim of the 3D calculations is to minimize the strength[3] of the allowed multipoles of the magnet by shaping the ends of the pole-pieces. The results from the 3D calculations of each 3D model were analyzed by expanding the radial field $B_r(r,z)$ calculated on a radius r=10 cm, { $B_r(r,z) = b_n(r,z)\cos[(n+1)\theta]$ n=1 quad n=3 oct …} and expansion

[3] Relative to the strength of the quadrupole multipole.

coefficients $b_n(r,z)$ that correspond to the various multipoles were compared among the various 3D models.

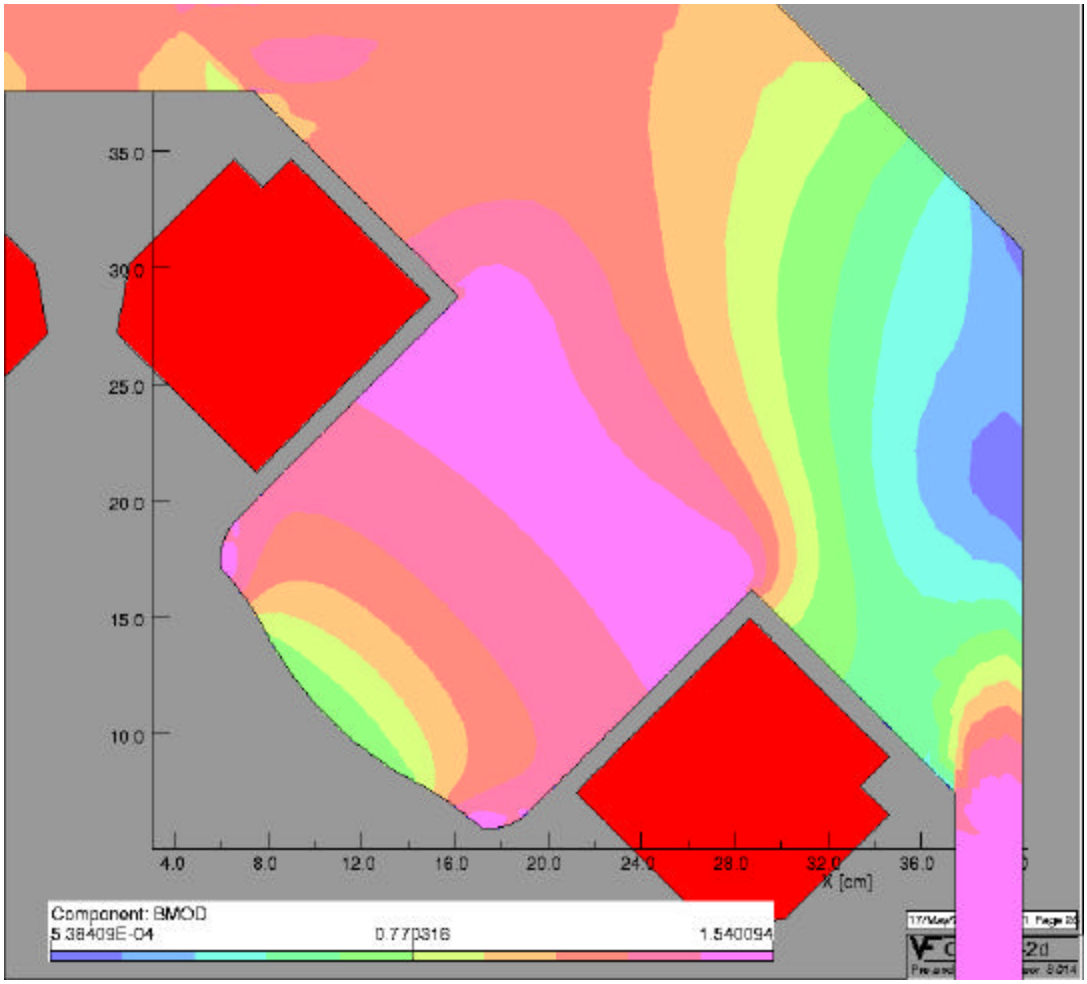

Figure 7. Contour plot of the B_{mod} in the iron of the quadrupole. The maximum value of B_{mod} does not exceed 16. kGauss.

In particular, the calculated coefficient of expansion $b_5(r,z)$ which is a measure of the strength of the dodecapole multipole is plotted as a function of the distance z from the center of the quadrupole in Fig. 8 for two 3D models a) No "pole-piece chamfer"[4] and b) with 30.25^o pole-pice chamfer[5] (see Fig. 9).

The strong variation of the b_5 coefficient plotted in Fig. 7 as a function of distance z is due to the end effects of the magnet.

In order to set a basis for comparison with the experimentally measured quantities, we calculated the values of the ratios $R_n = b_n(r,z)dz / b_1(r,z)dz$ where $b_n(r,z)dz$ is the amplitude of the radial field $b_n(r,z)$ of the n^{th} multipole, integrated along the z-direction at a radius r=10 cm.

[4] The cross section of the pole piece of the 3D model is identical to the cross section of the 2D model.

[5] The ends of the pole pieces have been chamfered by 30.25^o. The chamfer starts 6 cm from the edge of the pole face.

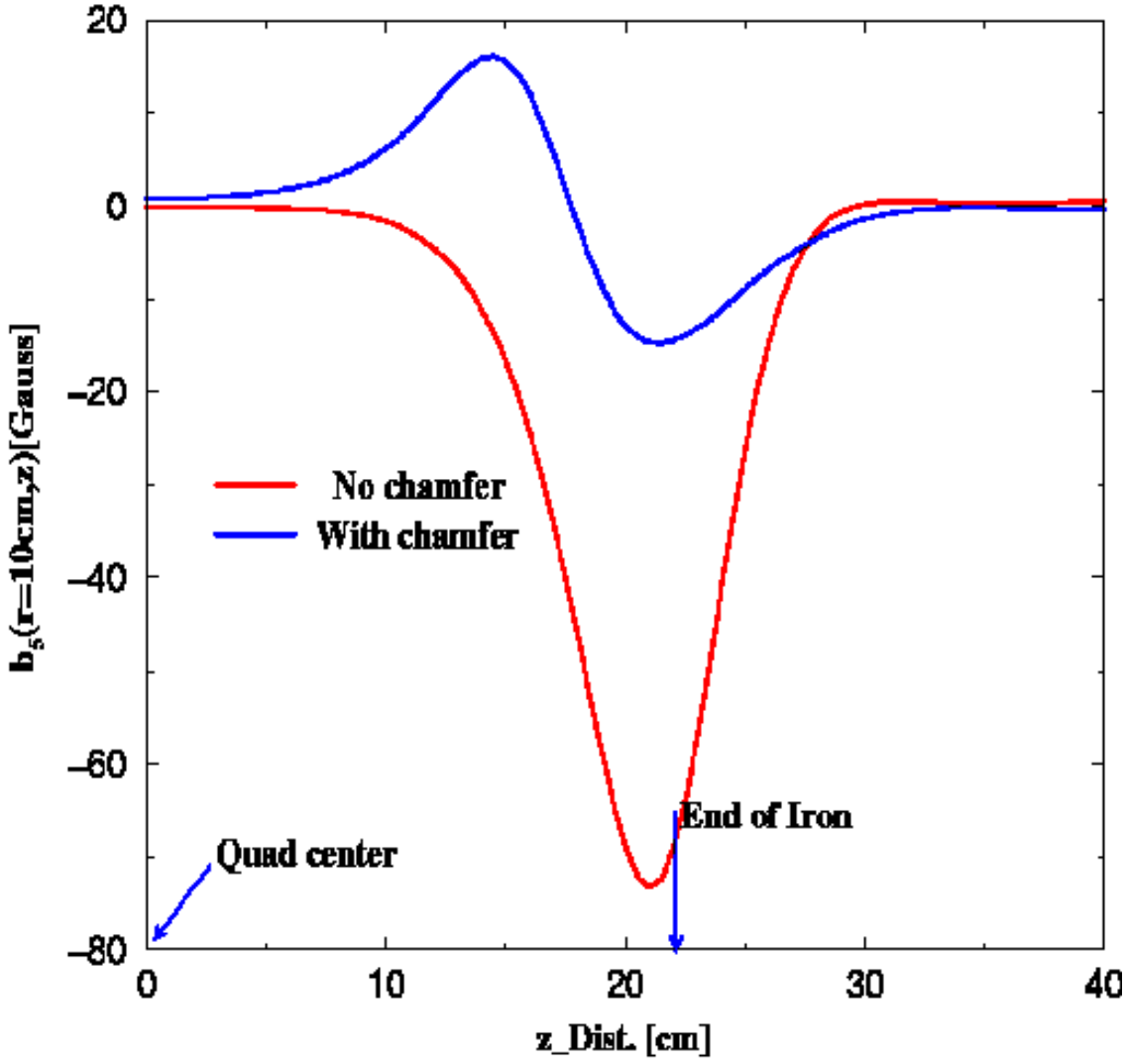

Figure 8. Plots of the expansion coefficient $b_5(r,z)$ at r=10cm as a function of distance z from the center of the quadrupole. The integral $b_h(r,z)dz$ is minimized by chamfering the end of the pole pieces as shown in Fig. 8.

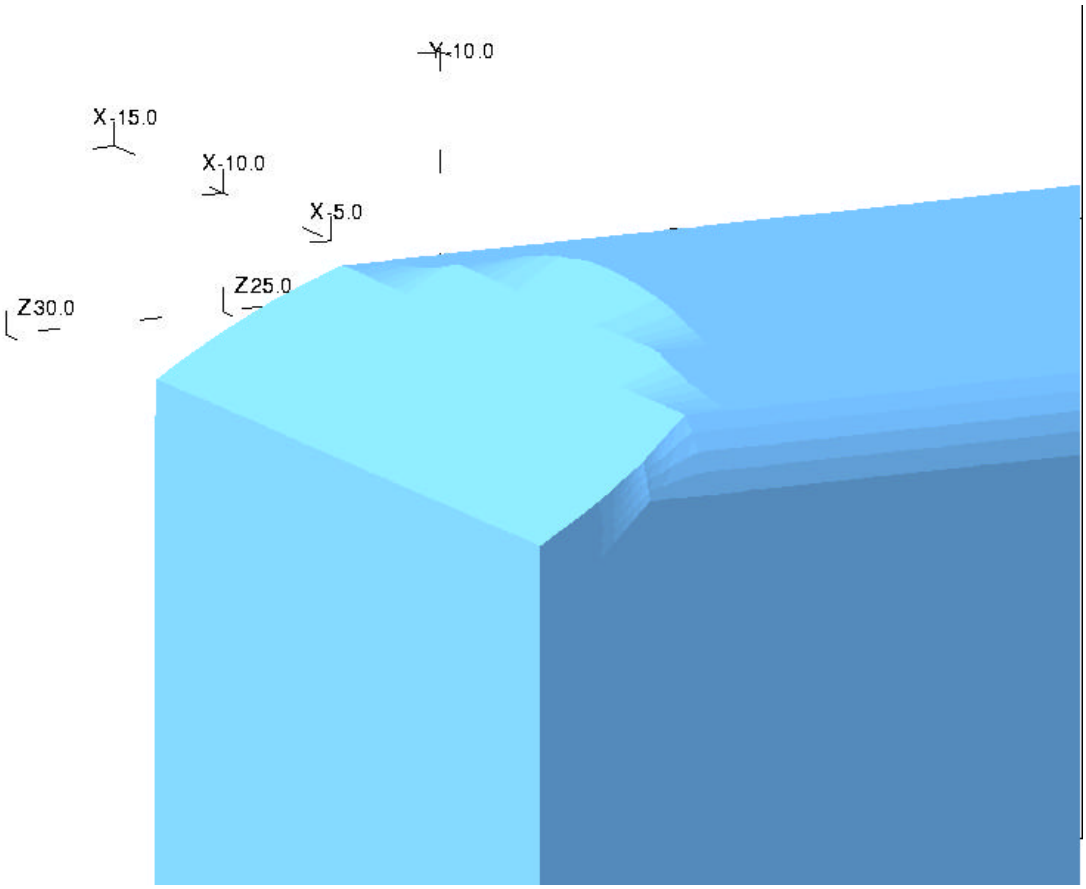

Figure 9. An isometric view of the chamfered end of one of the pole-piece of the quadrupole. The $b_5(r=10,z)$ coefficient for a chamfer of 30.25^o is plotted in Fig. 8. For this particular chamfer the value of $\int b_5(r,z)dz$ is minimized.

Table 3 contains the values of the calculated ratios R_n for the various multipoles and the ratios can be compared with the measured values. All value of the ratios R_n shown in Table 3 shows the ratio R_n of integrated strengths of the various allowed multipoles to the integrated quadrupole strength for a quadrupole chamfered by 30.25^o.

Table 3 are well below the upper limit of 2×10^{-4} except the value of the ratio [6] R_5 for the case of 1.3 GeV.

T [GeV]	$R_{3\ oct}$	$R_{5\ dod}$	$R_{7\ 16pole}$	L_{eff}
1.0	-8×10^{-6}	6×10^{-5}	-2×10^{-7}	53.3
1.3	-4×10^{-5}	5×10^{-4}	-2×10^{-6}	53.1

[6] Calculations show that an alternative 3D model that generates a ratio R5 ~2×10^{-4} at 1.0GeV excitation, can generate a ratio R_5 ~3×10^{-4} for excitation energy of 1.3 GeV. However we have chosen to use the model that generates the values of the R_n shown in Table 3.

Mechanical tolerances

The 3D modeling also provides an upper limit in the mechanical tolerances within which the magnet still satisfies the field requirements, thus avoiding "over or under"-design of the magnet. The mechanical tolerances were studied in a full 3D model by introducing possible mechanical errors in the dimensions of the 3D model.

a) An error of 0.5 mm in the longitudinal length of one of the poles of the magnet.
b) Rotation of a single pole-face by 1.5 mrad about an axis parallel to the symmetry axis of the quadupole and passing through the pole tip.

In both cases (a) and (b) above the variation of the ratio R_5 was ~10% of the value shown in Table 3, with the rest of the ratios maintaining still small values as those in Table 3.

Conclusions

Magnetic field calculations on 2D and 3D models of a large aperture narrow quadrupole provided optimum pole shape and dimensions for an SNS ring quadrupole which satisfies the field requirements of the SNS ring.
Upper limits on the mechanical tolerances were obtained by introducing mechanical errors on a full 3D-model.

* SNS is managed by UT-Battelle, LLC, under contract DE-AC05-00OR22725 for the U.S. Department of Energy. SNS is a partnership of six national laboratories: Argonne, Brookhaven, Jefferson, Lawrence Berkeley, Los Alamos, and Oak Ridge.

References

[1] J. Wei, et. al. Phys. Rev. ST Accel. Beams **3**, 080101 (2000)
[2] J. Wei, et. al. EPAC2000, p. 2560 Vienna, Austria
[3] N. Tsoupas et al. EPAC2000 p. 2270 Vienna, Austria
[4] Catalan-Lasheras et. al. EPAC2000 Rev. ST-AB **4**, 010101
[5] A. Fedotov et al. EPAC2000 p. 1492 Vienna, Austria
[6] Vector-Fields-Inc.
[7] D. Abell, et al. EPAC2000 p. 2107 Vienna, Austria